

## EFFECT OF TITANIUM, COPPER AND IRON ON SILICON SOLAR CELLS

A. ROHATGI, J. R. DAVIS, R. H. HOPKINS, P. RAI-CHOUDHURY and P. G. McMULLIN  
Westinghouse R&D Center Pittsburgh, PA 15235, U.S.A.

and

J. R. McCORMICK  
Hemlock Semiconductor Corporation, Hemlock, MI 48626, U.S.A.

(Received 22 February 1979; in revised form 4 April 1979)

**Abstract**—The effect of Ti, Cu and Fe on silicon solar cells has been investigated. Ti severely degrades cell performance above a concentration of  $10^{11} \text{ cm}^{-3}$ . The presence of  $2 \times 10^{14} \text{ cm}^{-3}$  Ti results in a 63% loss in cell performance and more than an order of magnitude reduction in carrier lifetime. Ti gives rise to two deep levels in Si at  $E_v + 0.30 \text{ eV}$  and  $E_c - 0.27 \text{ eV}$ . Copper, at concentrations below  $10^{16} \text{ cm}^{-3}$ , has negligible effect on cell performance and carrier lifetime. Above  $10^{16} \text{ cm}^{-3}$  copper occasionally produces a 10–15% loss in cell performance with a noticeable increase in junction excess current. No recombination centers were found due to Cu, instead considerable precipitation in the starting material was observed. Fe begins to hurt the cell performance above a concentration of  $2 \times 10^{14} \text{ cm}^{-3}$ . Iron at  $1.7 \times 10^{15} \text{ cm}^{-3}$  results in 46% loss in cell efficiency and about an order of magnitude reduction in lifetime. Fe induces a deep level in silicon at  $E_v + 0.4 \text{ eV}$ . The active center density, for both Ti and Fe, is only a very small fraction of the total impurity content in the starting silicon wafer.

### 1. INTRODUCTION

Large scale utilization of silicon photovoltaic devices requires low cost silicon. One way to accomplish this is to use cheaper, less pure silicon for the devices. For this reason, the tolerable impurity concentrations which do not degrade cell performance, have been determined for a number of impurities. The impurities studied are those usually found in partially refined silicon or might be incorporated during cell processing [1]. This paper presents a detailed examination of the effects of titanium, copper and iron on solar cell performance.

The impurities in silicon can influence the solar cell performance in a variety of ways. Crystal growth can be affected resulting in defects, inclusions, precipitates and structural breakdown [2]. Impurity induced recombination centers reduce the minority carrier lifetime in the silicon [3, 4]. Additional possible impurity related mechanisms include contact resistance effects, changes in series or shunt resistance [5] and increased junction excess current [6, 15] due to precipitates or other defects in the space charge region. Boron doped Czochralski single crystals were grown with controlled additions of Ti, Cu and Fe as secondary impurities and their concentrations were determined by emission and mass spectrographic techniques.  $n^+p$  solar cells were fabricated by a diffusion process. Cell performance parameters and carrier lifetimes were determined. Detailed I-V analysis, deep level transient spectroscopy and X-ray topography were performed to delineate the impurity effects.

### 2. EXPERIMENTAL

#### 2.1 Crystal growth

All ingots were prepared using the following nominal growth parameters;

pull rate	7 cm/hr
seed rotation	10–15 rpm CW

crucible rotation	2–4 rpm CCW
charge weight	869 gms (agv)
ingot diameter	3.3 cm
atmosphere	1 atm argon.

The ingots were nominally 4  $\Omega$ -cm, (111) boron doped. The secondary impurity concentration was in the range of  $10^{11}$ – $10^{17} \text{ cm}^{-3}$ . The upper limit was determined by solubility limitations and the tendency of the melt to become constitutionally supercooled with consequent polycrystalline growth.

#### 2.2 Metal impurity analysis

Spark source mass spectrometry was the primary tool used for the impurity analysis. These measurements have been supplemented, in selected instances, by neutron activation analysis. Generally, there was a good agreement between the target concentration and analytical data. The concentrations quoted are correct within a factor of 2.

#### 2.3 Solar cell fabrication

Solar cells were fabricated by a conventional process. The precleaned chem-polished wafers were phosphorous diffused at 825°C for 50 min which resulted in a sheet resistance of 60 ohms/square and a junction depth of approximately 0.35 microns. 1 cm  $\times$  1 cm cells were mesa etched and metallized with Ti-Pd-Ag using an electron beam system. The front pattern was a five-finger grid with 5.4% area coverage. The back surface was lapped prior to the metallization to ensure good ohmic contact.

Contacts were sintered at 550°C for 15 min in hydrogen. The cells were fabricated without back surface field or antireflecting coating. The average efficiency of baseline cells (no added secondary impurity) was about 10%. The usual experimental run consisted of 10–15 wafers from the impurity doped ingots along with 5–8 baseline wafers.

## 2.4 Solar cell characterization

Current–voltage measurements were made under illumination from a quartz-iodine simulator. The light level was set at 91.6 mW/cm<sup>2</sup> for the AM1 spectrum. The lighted I–V data was analyzed by a computer program using a single-exponential model

$$I = I_L - I_0[\exp((V + IR_s)/nV_T) - 1] \quad (1)$$

where  $V_T$  is the thermal voltage ( $kT/q$ ) and  $I_L$  is the photocurrent. The fit gives the parameters  $I_0$ ,  $R_s$ , and  $n$ . The peak power point ( $V_p$ ,  $I_p$ ) was determined by the solution of the following condition

$$\frac{dP}{dI} = I(dV/dI) + V = 0. \quad (2)$$

The cell efficiency was then determined by;

$$\text{eff}(\eta) = \frac{V_p \times I_p \times 100}{91.6 A_0} \quad (3)$$

where  $A_0$  is the total area of the cell.

## 2.5 I–V Analysis

The I–V characteristic of a  $p$ – $n$  junction solar cell is a composite of two exponential functions and resistance effects. These components must be separated from the measured I–V data in order to characterize the specific nature of impurity effects. The shunt resistance can be approximately determined from a reverse bias measurement [5] at  $V_R$  of 0.5–1 V

$$R_{sh} = V_R/I_R. \quad (4)$$

The series resistance,  $R_s$ , can be obtained from lighted and dark I–V data. The I–V relationship under illumination can be approximated by

$$V + IR_s = nV_T \cdot \ln((I_L - I)/I_0 + 1) \quad (5)$$

and in the dark by

$$V - IR_s = nV_T \cdot \ln(I/I_0 + 1) \quad (6)$$

where  $V$  and  $I$  are the magnitude of terminal voltage and current. Under the open circuit conditions equation (5) becomes

$$V_{oc} = nV_T \cdot \ln(I_L/I_0 + 1) \quad (7)$$

and in dark if we measure  $V_1$  at  $I = I_L$  eqn (6) becomes

$$V_1 - I_L R_s = nV_T \cdot \ln(I_L/I_0 + 1) \quad (8)$$

eqns (7) and (8) give

$$R_s = \frac{V_1 - V_{oc}}{I_L}. \quad (9)$$

Having determined  $R_{sh}$  and  $R_s$  their effect can be

removed by the following transformations

$$V' = V - IR_s \text{ and } I' = I - I_{sh}. \quad (10)$$

The dark characteristics can now be approximated by the sum of two exponential functions, one representing the base controlled current ( $I_b$ ) and other  $I_j$ , associated with the junction depletion region.

The base component [7]

$$I_b = I_{01} (\exp(V/V_T) - 1) \quad (11)$$

where

$$I_{01} = \frac{Aqn_i^2}{N_A} \sqrt{\left(\frac{D_n}{\tau_n}\right)}$$

for  $n^+p$  device with wide base. Notice the ideality factor  $n$  is unity in accord with theory [4, 7].

The junction current

$$I_j = I_{02} (\exp(V/nV_T) - 1), \quad (12)$$

for a recombination center in the middle of the band gap [6, 8]  $I_{02} = Aqn_i W_{dep}/2\tau_{dep}$  and  $n \approx 2$ . From the double exponential  $I_b$  and  $I_j$  can be separated numerically or graphically [9], recognizing that below about 0.3 V the total current,  $I_x$ , is nearly  $I_j$  so  $I_b$  can be obtained by extrapolating  $I_j$  and subtracting it from  $I_x$ .

$$I_b(V) = I_x(V) - I_j(V) \text{ for } V > 0.3 \text{ V}. \quad (13)$$

Operating point of the solar cell lies near 0.5 V therefore a slight displacement of the bulk current component on the log I–V plot can significantly alter cell performance, while  $I_j$  will have to slide up considerably to produce a comparable effect. A reduction in the base carrier lifetime is observed as a shift of the bulk current component to the left on the I–V plot. The transformed I–V plots, consisting of  $I_b$  and  $I_j$ , will be used to examine the impurity effect on the junction and the bulk.

## 2.6 Deep Level Transient Spectroscopy (DLTS)

DLTS measurements were performed using a double boxcar integrator as described by Lang [10] and Miller *et al.* [11]. A pulse ranging from  $-8$  to  $-2$  V and 100  $\mu$ s in duration was used to study the majority carrier traps and  $-8$  to  $+2$  V pulse was used to detect the minority carrier traps. The rate window [11] was controlled by changing the boxcar time-base from 0.5 to 100 msec while the gate delays,  $t_1$  and  $t_2$ , were set at 10 and 90% of the time base. For the DLTS studies, 1 cm<sup>2</sup> solar cell was subdivided into 30 mil diameter mesa diodes with a Ti–Au contact on the front and Ti–Pd–Ag at the back.

## 2.7 X-ray topography

The internal fine structure of wafers was revealed by means of x-ray extinction topographs formed by the Lang technique [12]. The study was conducted on wafers containing  $2 \times 10^{14}$  cm<sup>−3</sup> Ti,  $1.9 \times 10^{16}$  cm<sup>−3</sup> Cu,  $1.7 \times$

$10^{15} \text{ cm}^{-3} \text{ Fe}$  and a baseline wafer containing no intentionally added impurity. All traces of saw damage were removed by chemically polishing 3 mils from each surface of the wafers to produce a final wafer thickness of 10 mils. The wafers were traversed at 0.5 cm/min through a 2.5 cm high ribbon X-ray beam so that about 80% of the wafer area was imaged in a topograph. All exposures were made with  $\text{MoK}_{\alpha 1}$  radiation and recorded on Ilford G5 nuclear plates. Both the asymmetric (111) and symmetric (110) crystal reflections from the silicon were used; data for the former illustrate most of the significant features and are reported here.

### 3. RESULTS

The effect of controlled additions of titanium, copper and iron on cell performance and carrier lifetime are summarized in Table 1 and Fig. 1. The cell efficiencies are normalized with respect to the baseline cell efficiency (no added impurity) in each run. The impurities show a threshold concentration beyond which loss of cell efficiency becomes noticeable. Ti has the lowest threshold concentration, approx.  $3 \times 10^{11} \text{ cm}^{-3}$ . Titanium, at a concentration of  $2 \times 10^{14} \text{ cm}^{-3}$ , results in a 63% loss

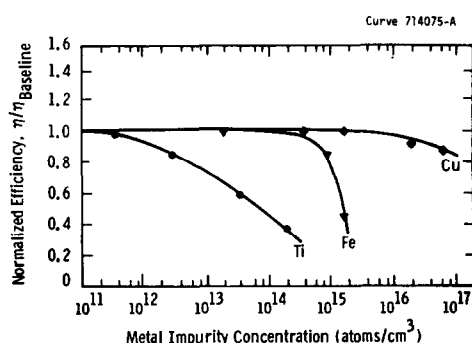


Fig. 1. Normalized silicon solar cell efficiency vs the content of titanium, copper or iron in the silicon.

in the cell efficiency and more than an order of magnitude reduction in the carrier lifetime. Copper shows a very large threshold concentration,  $\sim 2 \times 10^{15} \text{ cm}^{-3}$ , and beyond this level it only has a very small effect on the cell performance. At a concentration of  $6.5 \times 10^{16} \text{ cm}^{-3} \text{ Cu}$ , a scatter in the cell performance is observed which ranges from 85 to 100% of the baseline performance. Short-circuit current remains unaffected by Cu but lower efficiency cells show high junction excess current. Fe has an intermediate threshold concentration of  $2 \times 10^{14} \text{ cm}^{-3}$  beyond which it shows a rapid degradation in the cell performance.  $1.7 \times 10^{15} \text{ cm}^{-3} \text{ Fe}$  results in 46%

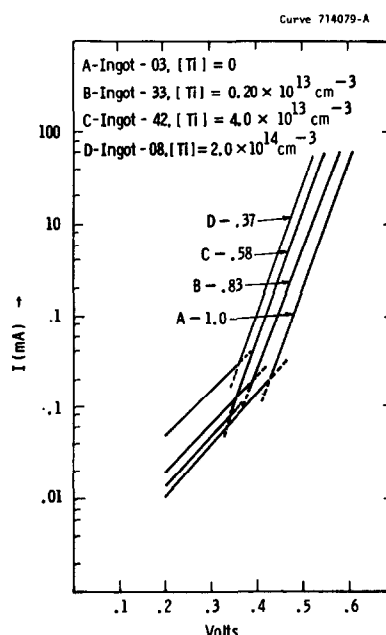


Fig. 2. Transformed dark  $I$ - $V$  curves for titanium-doped  $4 \Omega\text{-cm}$  silicon solar cells. Each curve is labelled with normalized cell efficiency.

Table 1. Effect of titanium, copper and iron on silicon solar cell performance and OCD lifetime

Ingot ID	Impurity Concentration # $\text{cm}^{-3}$	Normalized Cell Efficiency $\eta/\eta_{\text{BL}}$	Open Circuit Decay Lifetime ( $\mu\text{sec}$ )*
BL-03	0	1.0	4.5
Ti-48	$3.6 \times 10^{11}$	0.98	3.97
Ti-33	$2.0 \times 10^{12}$	0.83	2.02
Ti-42	$4.0 \times 10^{13}$	0.58	0.53
Ti-08	$2.0 \times 10^{14}$	0.37	0.17
Fe-44	$1.3 \times 10^{13}$	1.0	4.3
Fe-16	$9.0 \times 10^{14}$	0.86	2.6
Fe-18	$1.7 \times 10^{15}$	0.54	0.3
Cu-07	$1.7 \times 10^{15}$	1.0	3.7
Cu-17	$1.9 \times 10^{16}$	0.91-1.0	3.0
Cu-56	$6.5 \times 10^{16}$	0.85-1.0	3.4

\* Current density used in the open circuit voltage decay measurement was  $20 \text{ mA/cm}^2$ .

# Impurity concentration is the total and not the active.

loss in the cell efficiency and about an order of magnitude reduction in the lifetime.

The  $I$ - $V$  curves for Ti, Cu and Fe doped cells have been transformed as discussed in Section 2.5 and are shown in Figs. 2, 3 and 4 respectively. These curves reveal that Ti primarily lowers the bulk lifetime and has only a small effect on the junction response at high concentration. Copper has negligible effect on the bulk but occasionally affects the junction response and the  $I$ - $V$  curves of such samples are shown in Fig. 3. The  $I$ - $V$  curve looks very similar to the baseline when the junctions are not affected. Fe initially affects the bulk only but above concentrations of  $10^{15} \text{ cm}^{-3}$  it shows appreciable influence on the junction response, with some scatter. Such an example is shown in Fig. 4.

At these concentrations, impurities did not alter the shunt and series resistances enough to account for appreciable loss in the cell performance. In most cases  $R_{sh}$  was above  $15 \text{ k}\Omega$  and  $R_s$  about  $0.5 \Omega$  ( $1 \text{ cm}^2$  cells).

Figure 5 shows the x-ray topographs of the baseline wafer along with wafers containing  $1.9 \times 10^{16} \text{ cm}^{-3}$  Cu and  $2 \times 10^{14} \text{ cm}^{-3}$  Ti. The topographs indicate that both the metal-bearing and baseline crystals exhibit the same gross features. Each contain dislocation arrays distributed fairly uniformly over the crystal diameter. The dislocation densities were typically  $10^3 \text{ cm}^{-2}$  and these defects were preferentially aligned in  $\langle 110 \rangle$  directions with numerous indications of dislocation interactions, as is common in silicon [13].

While the overall features were similar, the topographs at  $20\times$  magnification indicated some distinct differences depending on the metal impurity present. Figure 5(a) shows that the uncontaminated baseline wafer has many long straight dislocation segments, sharply imaged with no evidence for decoration. In contrast, a wafer containing a fast diffusing species like Cu show considerable

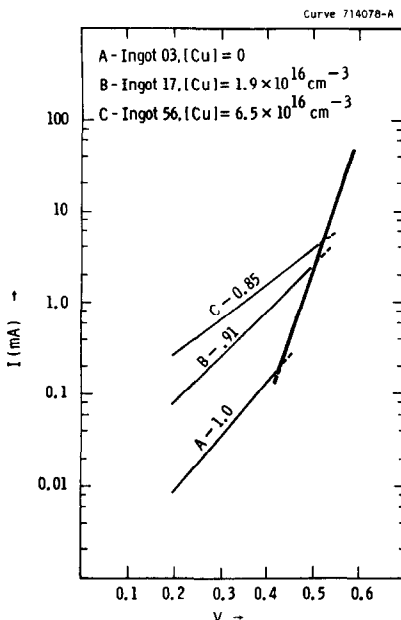


Fig. 3. Transformed dark  $I$ - $V$  curves for copper-doped  $4\text{-}\Omega\text{-cm}$  silicon solar cells. Each curve is labelled with normalized cell efficiency.

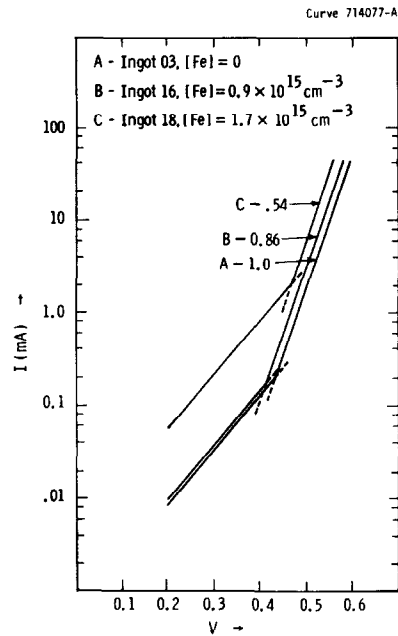


Fig. 4. Transformed dark  $I$ - $V$  curves for iron-doped  $4\text{-}\Omega\text{-cm}$  silicon solar cells. Each curve is labelled with normalized cell efficiency.

decoration of the dislocation lines by precipitates. Precipitation indeed is so heavy in the Cu-doped wafer that the normal X-ray extinction conditions are modified to a point where the dislocation lines themselves virtually disappear, only the strain fields of precipitates being imaged as in Fig. 5(b). The precipitates appear as a row of dark dots marking the position of the original dislocation line. The topograph for the titanium-doped crystal, Fig. 5(c) gives no evidence for precipitation. The dislocation arrays are similar to those of the baseline ingot (some of the images are fringed where the dislocations outcrop on the wafer surface). Topographs for the iron-doped crystal (not shown) appeared much like those for the titanium-doped crystal except that many areas along the dislocations showed enhanced diffraction contrast. There was insufficient resolution on the X-ray plates from the iron-doped crystal to determine whether or not this extra contrast was due to precipitation as in the case of the copper-doped crystals.

Figure 6 shows the plot of emission rate, adjusted for the  $T^2$  dependence of  $N_c V_{th}$ , as a function of temperature for the deep levels obtained from DLTS measurements. Ti induced deep levels at  $E_v + 0.30 \text{ eV}$  and  $E_c - 0.27 \text{ eV}$  and the corresponding recombination center densities were  $3.5 \times 10^{13} \text{ cm}^{-3}$  and  $1.5 \times 10^{13} \text{ cm}^{-3}$ . No recombination centers were detected in the Cu-doped samples. Data from the iron-doped cells indicate a deep level at  $E_v + 0.4 \text{ eV}$  with a trap density of  $1 \times 10^{13} \text{ cm}^{-3}$ .

#### 4. DISCUSSION

Figure 1 shows that Ti is very harmful to  $p$ -base silicon solar cells. Above a concentration of  $3 \times 10^{11} \text{ cm}^{-3}$  it degrades the cell performance primarily by lowering the bulk lifetime. At  $2 \times 10^{14} \text{ cm}^{-3}$  Ti produces a 63% loss in the cell performance and more than an order of magnitude reduction in the carrier

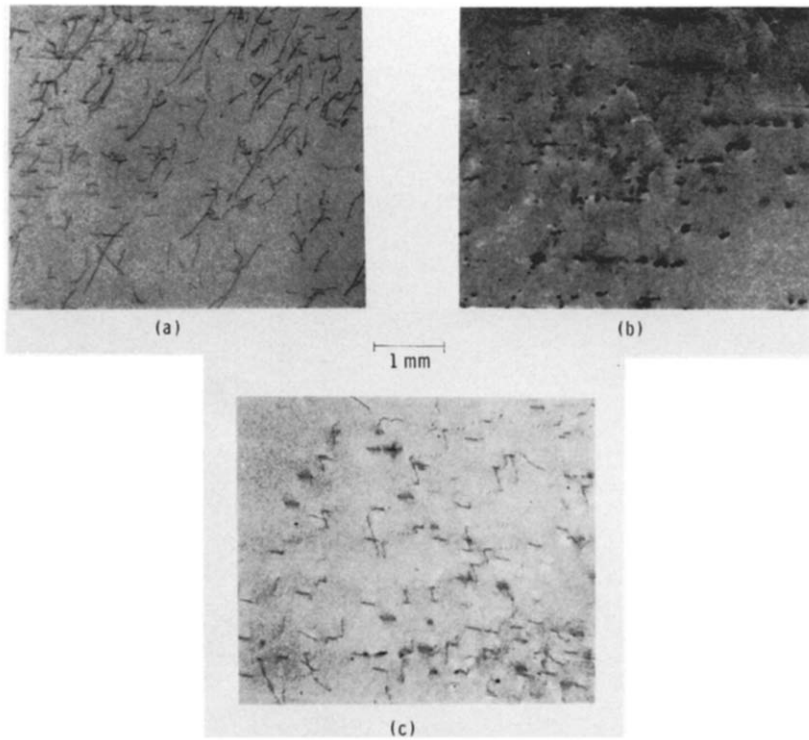


**Fig. 5.** X-ray topographs of (111) silicon single crystals at 20 $\times$  magnification (a) baseline crystal, (b) crystal doped with  $2 \times 10^{16} \text{ cm}^{-3}$  Cu, (c) crystal doped with  $2 \times 10^{14} \text{ cm}^{-3}$  Ti.



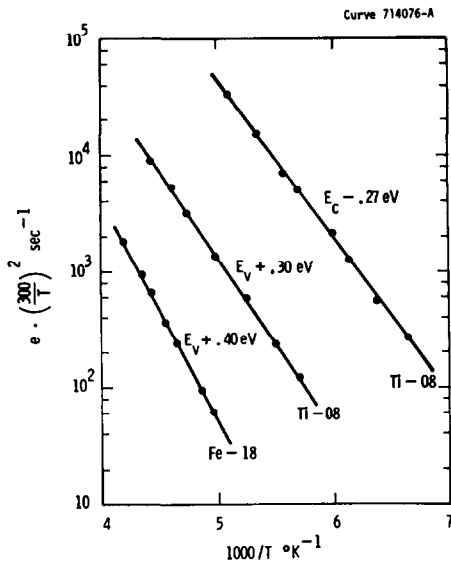


Fig. 6. Emission rate as a function of temperature for the traps observed in 4  $\Omega$ -cm *p*-type silicon containing  $2 \times 10^{14} \text{ cm}^{-3}$  Ti or  $1.7 \times 10^{15} \text{ cm}^{-3}$  Fe.

lifetime (Table 1). At high concentrations Ti begins to show some effect on junction excess current but not enough to account for an appreciable reduction in cell performance (Fig. 2). The concentrations of the induced recombination centers at  $E_v + 0.30 \text{ eV}$  and  $E_c - 0.27 \text{ eV}$ , obtained from DLTS, indicate that only a small fraction, 10–20%, of the total titanium present in the starting material is electrically active. No precipitates were observed in X-ray topograph of the starting material therefore it is not clear how to account for the large fraction of inactive titanium. Phosphorous diffusion during the junction formation may getter some titanium in the  $n^+$  region. However, Ti is not a fast diffuser in silicon so the extent of gettering is expected to be much smaller than for impurities like iron and copper [14]. Some investigations are being carried on Ti bearing float-zone silicon, which contains much less carbon and oxygen, to see if Ti interaction with oxygen and carbon can explain the inactivity.

Investigation of copper bearing samples show that  $10^{15}$ – $10^{16} \text{ cm}^{-3}$  Cu, present in the starting silicon wafer, has negligible effect on the solar cells fabricated by this process. At a Cu concentration of  $6.5 \times 10^{16} \text{ cm}^{-3}$ , the scatter in the cell performance ranges from 85 to 100% of the baseline efficiency. The lower efficiency cells show appreciable increase in the junction excess current, however the short-circuit current,  $I_{sc}$ , remains equal to that of the baseline in all cases.  $I_{sc}$  is a good indicator of the bulk lifetime which implies that the base is relatively free from Cu induced recombination centers. The increased junction excess current, which at the operating point represents a loss of photocurrent in the junction region, appears to be the sole reason for the lower efficiencies occasionally observed in heavily Cu-doped cells. The cell data is consistent with the DLTS response which showed no detectable trap centers in the base of solar cells containing  $1.9 \times 10^{16} \text{ cm}^{-3}$  copper. Some investigators [15] have reported three acceptor levels due

to Cu. Cu precipitates observed in the starting material, along with Salama's [16] observation that a considerable amount of Cu is getterd into precipitates in the  $n^+$  region may account for the lack of detectable traps in the base of these samples. If such precipitates exist in the depletion region or extend partially into the junction then they will give rise to the occasionally observed increase in the junction excess current. Crystal defects of this type are known to increase leakage current [17].

Iron is an undesirable impurity in *p*-base silicon solar cells. At  $1.7 \times 10^{15} \text{ cm}^{-3}$  Fe results in 46% loss in the cell performance. As the concentration increases above  $10^{15} \text{ cm}^{-3}$ , Fe produces irregular increases in the junction excess current which combined with the lifetime loss accounts for the rapid degradation in performance beyond the threshold. Regions of enhanced contrast in the x-ray topographs were insufficiently resolved to prove the presence of precipitates inferred on the basis of the junction current effect. A deep level at  $E_v + 0.4 \text{ eV}$  was found in the iron-doped samples which is in agreement with the other investigators [18, 19]. Like Ti, the concentration of the active iron center,  $1 \times 10^{13} \text{ cm}^{-3}$ , was a very small fraction of the total Fe,  $1.7 \times 10^{15} \text{ cm}^{-3}$ , present in the silicon again suggesting precipitation and/or gettering.

## 5. CONCLUSIONS

Titanium-induced loss of performance, above a concentration of  $\sim 3 \times 10^{11} \text{ cm}^{-3}$ , occurs primarily due to minority carrier recombination associated with two deep levels observed at  $E_v + 0.3 \text{ eV}$  and  $E_c - 0.27 \text{ eV}$ . At a Ti concentration of  $2 \times 10^{14} \text{ cm}^{-3}$ , the base lifetime is reduced by more than a factor of 10 and cell efficiency is reduced by 63%.

For iron, the threshold impurity concentration for cell degradation is  $\sim 2 \times 10^{14} \text{ cm}^{-3}$ . Above this level carrier lifetime is significantly reduced apparently by the presence of a level at  $E_v + 0.4 \text{ eV}$ . In contrast to titanium, iron above  $10^{15} \text{ cm}^{-3}$  induces additional cell performance loss believed to be due to precipitates in or near the junction depletion region. The measured density of recombination centers, for both iron and titanium, is a small fraction ( $< 20\%$ ) of the total metal content.

Copper results in a slight cell performance loss above a concentration of  $\sim 10^{16} \text{ cm}^{-3}$  which is entirely due to precipitate effects on the junction. No deep level or lifetime degradation was observed.

**Acknowledgements**—This work was performed as part of the Jet Propulsion Laboratory Low Cost Silicon Solar Array Project sponsored by the U.S. Department of Energy.

The authors wish to thank J. W. Chen, D. N. Schmidt, B. Westwood and H. F. Abt for their assistance in the experimental work.

## REFERENCES

1. J. R. Davis *et al.*, *Proc. 13th IEEE Photovoltaic Specialists Conf.* Washington, D.C., p. 490 (1978).
2. R. H. Hopkins *et al.*, *J. Crystal Growth* **42**, 493 (1977).
3. W. Shockley and W. T. Read, *Phys. Rev.* **107**, 392 (1957).
4. C. T. Sah, R. N. Noyce and W. Shockley, *Proc. IEEE*, **45**, 1228 (1957).

5. M. Wolf, H. Rauschenbach, *Solar Cells* 89 (Edited by C. E. Backus) IEEE Press, New York (1976).
6. R. J. Stirn, *Proc. 9th IEEE Photovoltaic Specialists Conf.*, Silver Springs, 72 (1972).
7. W. Shockley, *Bell Syst. Tech. J.* **28**, 435 (1948).
8. A. S. Grove, *Physics and Technology of Semiconductor Devices*. Wiley, New York (1967).
9. A. Neugroschel, F. Lindholm and C. T. Sah, *IEEE Trans. Electron. Dev.* **ED24**, 662 (1977).
10. D. V. Lang, *J. Appl. Phys.* **45**, 3023 (1974).
11. G. L. Miller, D. V. Lang and L. C. Kimerling, *Ann. Rev. Material Science*, 377 (1977).
12. A. R. Lang, *Acta Cryst.* **12**, 249 (1959).
13. A. E. Jenkinson and A. R. Lang, *Direct-observation of imperfections in crystals*, 471 Metallurgical Society of AIME, New York (1962).
14. M. Nakamura, T. Kato and N. Oi, *Jap. J. of Applied Physics* **7**(5), 512 (1968).
15. R. N. Hall and J. M. Racette, *J. Appl. Phys.* **35**, 379 (1964).
16. A. M. Salama, *Proc. of the Topical Conf. on Characterization Techniques for Semiconductor materials and devices*, **78-3**, 334 (1978).
17. J. E. Lawrence, *J. Elect. Chem. Soc.* **112**, 796 (1965).
18. C. B. Collins and R. O. Carlson, *Phys. Rev.* **108**, 1409 (1957).
19. J. W. Chen and A. G. Milnes, *Proc. of the National Workshop on Low Cost Polycrystalline Silicon Solar Cells* (Edited by T. L. Chu and S. S. Chu) (1976).